# *Ab initio* estimation of math xmlns="http://www.w3.org/1998/Math/MathML">mrow>mi>E/mi>mn>2/mn>/mrow>/math> strengths in math xmlns="http://www.w3.org/1998/Math/MathML">mmultiscripts>mi>Li/mi>mprescripts>/mprescripts>none>/none>mn>8/mn>/mmultiscripts>/math> and its neighbors by normalization to the measured quadrupole moment

Mark A. Caprio and Patrick J. Fasano

Phys. Rev. C **106**, 034320 — Published 26 September 2022

DOI: 10.1103/PhysRevC.106.034320

# *Ab initio* estimation of $E2$ strengths in $^8$Li and its neighbors by normalization to the measured quadrupole moment

Mark A. Caprio and Patrick J. Fasano

*Department of Physics and Astronomy, University of Notre Dame, Notre Dame, Indiana 46556-5670, USA*

(Dated: September 6, 2022)

For electric quadrupole ($E2$) observables, which depend on the large-distance tails of the nuclear wave function, *ab initio* no-core configuration interaction (NCCI) calculations converge slowly, making meaningful predictions challenging to obtain. Nonetheless, the calculated values for different $E2$ matrix elements, particularly those involving levels with closely-related structure (*e.g.*, within the same rotational band) are found to be robustly proportional. This observation suggests that a known value for one observable may be used to determine the overall scale of $E2$ strengths, and thereby provide predictions for others. In particular, we demonstrate that meaningful predictions for $E2$ transitions may be obtained by calibration to the ground-state quadrupole moment. We test this approach for well-measured low-lying $E2$ transitions in $^7$Li and $^9$Be, then provide predictions for transitions in $^8$Li and $^9$Li. In particular, we address the $2^+ \rightarrow 1^+$ transition in $^8$Li, for which the reported measured strength exceeds *ab initio* Green's function Monte Carlo (GFMC) predictions by over an order of magnitude.

## I. INTRODUCTION

Electric quadrupole ($E2$) observables provide key measures of nuclear collective structure [1–3], in particular, rotation and deformation. However, *ab initio* calculations for $E2$ observables are notoriously challenging to obtain [4–6]. Since $E2$ observables are sensitive to the large-distance tails of the nuclear wave function, they are slowly convergent in *ab initio* no-core configuration interaction (NCCI), or no-core shell model (NCSM), approaches [7], which conventionally rely upon an oscillator-basis expansion of the wave function. In practical calculations, the basis for the many-body space must be truncated to finite size. The results can therefore, at best, only approximate the $E2$ predictions which would be obtained by solving the full (untruncated) many-body problem for a given internucleon interaction. While one may attempt to improve the many-body calculation by various means (*e.g.*, Refs. [8–12]) so as to improve convergence of $E2$ observables, the accuracy is nonetheless severely limited by computational constraints.

We may thus, alternatively, seek indirect ways to circumvent the convergence challenges affecting $E2$ observables. In particular, the convergence patterns of calculated $E2$ matrix elements are often strongly correlated [13–18], especially for matrix elements involving states with similar structure. This suggests [14] that, if one $E2$ matrix element is well-known from experiment (or, in principle, a complementary *ab initio* calculation using an alternative many-body method), a meaningful prediction may then be made for another, correlated $E2$ matrix element. Calci and Roth [14] use the well-measured $E2$ strength between the ground state and first excited state, in $^6$Li and $^{12}$C, to obtain a prediction for the elusive excited-state quadrupole moment.

Conversely, in the present work, we demonstrate the viability of the ground-state quadrupole moment as a calibration reference by which to generate predictions of $E2$ strengths, through robust *ab initio* NCCI predictions of the dimensionless ratio $B(E2)/(eQ)^2$, in which systematic truncations errors in the calculated $E2$ matrix elements cancel. The ground-state quadrupole moment is well-measured for many nuclei [19], as summarized for $p$-shell nuclides in Fig. 1. Calibration to this observable is subject to the fundamental constraint that the ground state angular momentum must admit a nonvanishing quadrupole moment ($J \geq 1$), as well as practical constraints that measurement must be feasible [25], including that the ground state must be particle-bound.

The case of $^8$Li is of particular interest, as an instance in which this approach may be applied to obtain *ab initio* insight, given the anomalously enhanced strength reported for the transition between the $2^+$ ground state and $1^+$ first excited state of this nuclide. This $E2$ strength has been measured through Coulomb excitation of $^8$Li in a radioactive beam experiment, yielding $B(E2; 2^+ \rightarrow 1^+) = 55(15)\,e^2\mathrm{fm}^4$ [21, 26], or, in terms of the Weisskopf single-particle estimate [27], $\approx 58\,\mathrm{W.u.}$ (The gamma decay lifetime of the $1^+$ state instead yields only information on the $M1$ strength [21].) This is among the most enhanced $E2$ transition strengths reported in a $p$-shell nuclide [20–24]. Compare, *e.g.*, $B(E2; 3/2^- \rightarrow 1/2^-) \approx 10\,\mathrm{W.u.}$ for the analogous (upward) transition from the ground

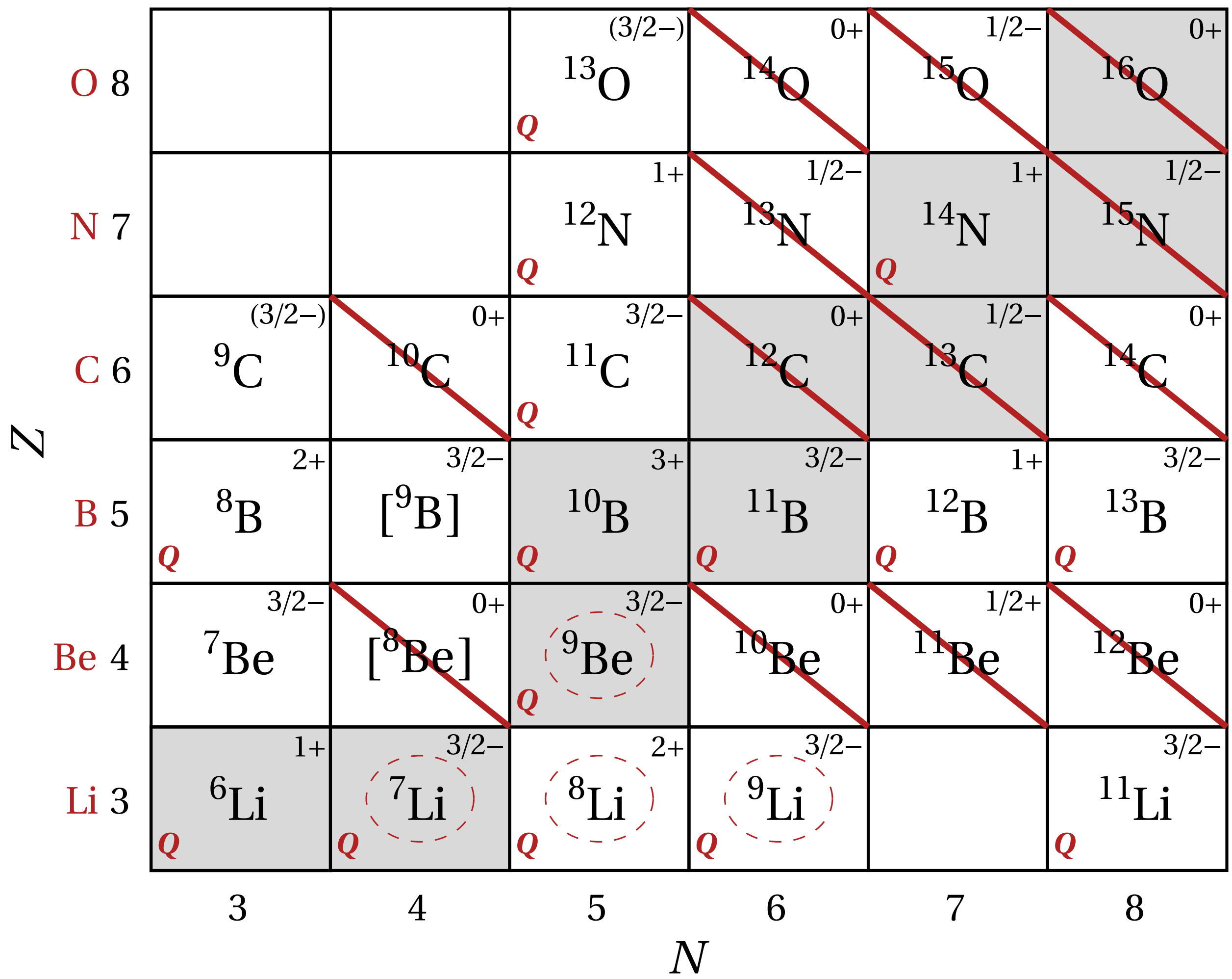


FIG. 1. Nuclides with measured ground-state quadrupole moments [19] (indicated with the letter "$Q$") in the $p$ shell. Particle-bound nuclides are designated by name, while brackets indicate a particle-unbound but narrow ($\lesssim 1\,\mathrm{keV}$) ground-state resonance, and shading indicates stable nuclides. The ground-state angular momentum and parity are given [20–24] (upper right), while slashes serve to exclude those nuclei (with $J \leq 1/2$) for which the ground-state angular momentum does not support a quadrupole moment. The nuclide $^8$Li and its neighbors considered in this work are highlighted (dashed circles). Figure adapted from Ref. [18].

state of neighboring $^7$Li [20], or $B(E2; 3/2^- \to 5/2^-) \approx 42\,\mathrm{W.u.}$ similarly in neighboring $^9$Be [24].

However, Green's function Monte Carlo (GFMC) calculations [28] give a predicted strength nearly two orders of magnitude smaller, at $0.83(7)\, e^2\mathrm{fm}^4$ [28]. Moreover, we note that such enhancement in $^8$Li would be particularly remarkable, given that it cannot be explained in terms of in-band rotational collectivity, while the aforementioned transitions in neighboring $^7$Li and $^9$Be are ostensibly rotational in nature [17]. Even if the $2^+$ ground state is taken to be a $K = 2$ rotational band head, this band would have no $J = 1$ member.

We first establish the expected form for the correlation between $B(E2)$ and quadrupole moment observables, through the dimensionless ratio $B(E2)/(eQ)^2$ (Sec. II), and demonstrate the robust convergence of this ratio for experimentally well-measured $E2$ transition strengths, between the ground state and first excited state (of the same parity), in $^7$Li and $^9$Be (Sec. III). We then return to the anomalous $2^+ \to 1^+$ transition in $^8$Li and other unmeasured $E2$ strengths to low-lying states in $^8$Li and $^9$Li (Sec. IV).

## II. DIMENSIONLESS RATIO

The $E2$ reduced transition probability depends upon the square of a reduced matrix element of the $E2$ operator, as

$$B(E2; J_i \to J_f) \propto |\langle J_f \| \, Q_2 \, \| J_i \rangle|^2, \tag{1}$$

while the quadrupole moment, originally defined in terms of the stretched matrix element $\langle JJ | \, Q_{2,0} \, | JJ \rangle$, is simply proportional to a reduced matrix element, as

$$eQ(J) \propto \langle J \| \, Q_2 \, \| J \rangle. \tag{2}$$

The sensitivity of each observable to the large-distance properties of the nuclear wave function arises from the $r^2$ dependence of the $E2$ operator [29], $Q_{2\mu} = \sum_{i \in p} e r_i^2 Y_{2\mu}(\hat{\mathbf{r}}_i)$, where the summation runs over the (charged) protons. The ratio

$$\frac{B(E2)}{(eQ)^2} \propto \left| \frac{\langle J_f \| Q_2 \| J_i \rangle}{\langle J \| Q_2 \| J \rangle} \right|^2 \tag{3}$$

is dimensionless, and involves like powers of reduced matrix elements of the $E2$ operator in the numerator and denominator. We thus have reason to hope for at least partial cancellation of the error arising in these matrix elements due to truncation of the nuclear wave functions.

## III. ILLUSTRATION FOR $^7$Li AND $^9$Be

In the NCCI approach, the true results of solving the many-body problem in the full many-body space would be obtained if the full, infinite oscillator basis could be used. However, for finite calculations, results depend upon the subspace spanned by the truncated basis. Thus they depend both upon the maximum number $N_{\mathrm{max}}$ of oscillator excitations allowed within the configurations making up the many-body basis, and upon the oscillator length of the underlying single-particle states (or, equivalently, the oscillator parameter $\hbar\omega$ [29]). Convergence is recognized when the calculated results become insensitive to increases in $N_{\mathrm{max}}$ and to variation in $\hbar\omega$ (see, *e.g.*, Refs. [4, 5, 17]).

Let us first consider the convergence of the calculated $3/2^- \rightarrow 1/2^-$ $E2$ strength for $^7$Li, shown in Fig. 2(a), as obtained using the Daejeon16 internucleon interaction [30]. This interaction is based on the two-body part of the Entem-Machleidt N$^3$LO chiral effective field theory ($\chi$EFT) interaction [31], softened via a similarity renormalization group (SRG) transformation [32] so as to provide comparatively rapid convergence, and then adjusted via a phase-shift equivalent transformation to better describe nuclei with $A \leq 16$ while still maintaining rapid convergence. Calculations are carried out using the NCCI code MFDn [33–35]. (Comprehensive plots and tabulations of calculated observables, as functions of $N_{\mathrm{max}}$ and $\hbar\omega$, are provided in the Supplemental Material [36].)

The values along each curve in Fig. 2 represent the results of calculations carried out with the same basis truncation $N_{\mathrm{max}}$ (from short dashes for $N_{\mathrm{max}} = 4$ to solid lines for $N_{\mathrm{max}} = 16$) and differing $\hbar\omega$. While there is perhaps some tendency towards flattening of these curves with respect to $\hbar\omega$ ("shouldering") and compression of successive curves with respect to $N_{\mathrm{max}}$, the calculated values are still steadily increasing with increasing $N_{\mathrm{max}}$. At best, we might crudely estimate the true value which would be obtained for the given internucleon interaction in the full, untruncated many-body space.

A similar convergence pattern is found for the calculated $3/2^-$ ground state quadrupole moment [Fig. 2(d)], where, however, the curves are inverted due to the negative sign on the quadrupole moment. (For further discussion of the convergence of this and other quadrupole moments in NCCI calculations, see Ref. [18].) With each increment in $N_{\mathrm{max}}$, the relative (fractional) change between calculated values of the quadrupole moment is smaller than for the $B(E2)$. This is to be expected, as the quadrupole moment is simply proportional to a

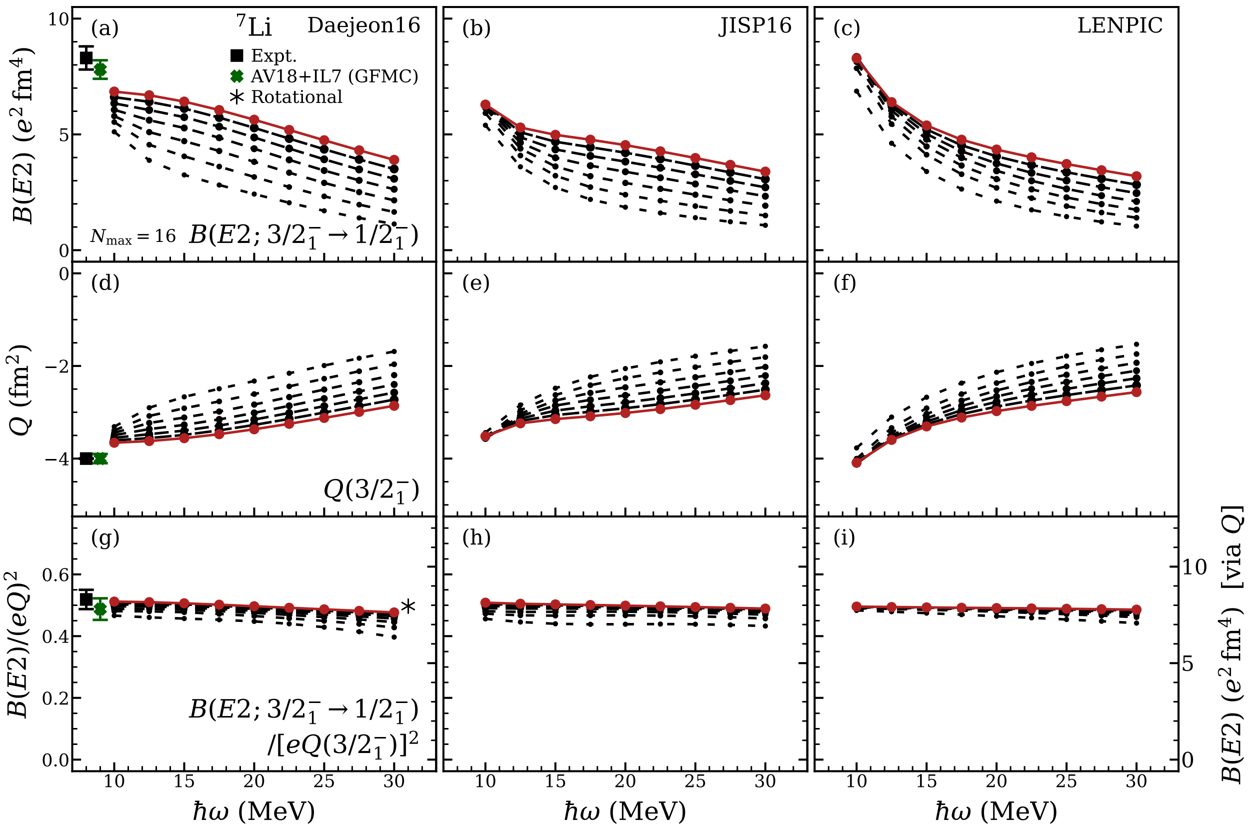


FIG. 2. Convergence of *ab initio* NCCI calculated observables for $^7$Li: (top) the $3/2^- \to 1/2^-$ $E2$ strength, (middle) the electric quadrupole moment of the $3/2^-$ ground state, and (bottom) the dimensionless ratio $B(E2)/(eQ)^2$ constructed from the preceding two observables. Results are shown for the (left) Daejeon16, (center) JISP16, and (right) LENPIC interactions. When calibrated to the experimental quadrupole moment, the ratio provides a prediction for the absolute $B(E2)$ (scale at right). Calculated values are shown as functions of the basis parameter $\hbar\omega$, for successive even value of $N_{\mathrm{max}}$ (increasing symbol size and longer dashing), from $N_{\mathrm{max}} = 4$ (short dashed curves) to 16 (solid curves). For comparison, experimental values [19, 20] (squares), GFMC AV18+IL7 predictions [28] (crosses), and the rotational ratio (asterisk) are also shown.

matrix element of the $E2$ operator, while the $B(E2)$ is proportional to the square of such a matrix element, and (as in elementary error analysis) squaring a quantity doubles relative changes in that quantity. However, one may again at best attempt a crude estimate of the value which would be obtained in the full, untruncated many-body space.

In $^7$Li, both the $E2$ strength and the quadrupole moment are known experimentally, with measured values of $B(E2; 3/2^- \to 1/2^-) = 8.3(5)\, e^2\mathrm{fm}^4$ [20] and $Q(3/2^-) =$

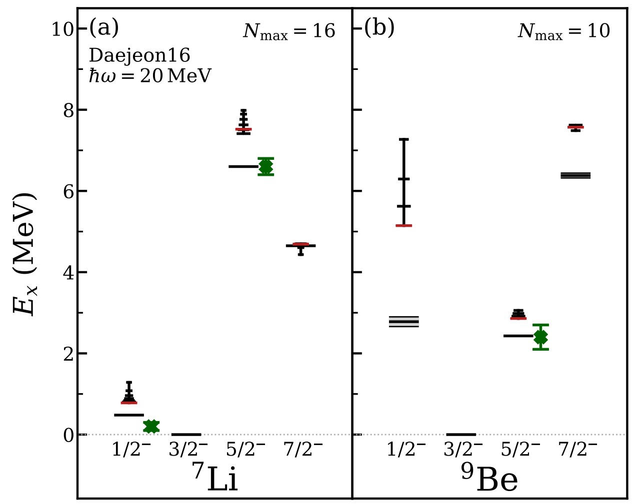


FIG. 3. Calculated excitation energies of low-lying states in (a) $^7$Li and (b) $^9$Be, with angular momentum and parity as indicated at bottom, as obtained with the Daejeon16 interaction. Calculated values are shown at fixed $\hbar\omega = 20\,\mathrm{MeV}$ and varying $N_{\max}$ (increasing symbol size), from $N_{\max} = 4$ to the maximum value indicated (at top). Experimental energies [20, 21] are shown (horizontal line and error band) where available, as are the GFMC AV18+IL7 predictions [28] (crosses) (see Table III of Ref. [37]).

$-4.00(3)\,\mathrm{fm}^2$ [19, 20] (squares in Fig. 2). While the NCCI calculated values for both the $B(E2)$ [Fig. 2(a)] and quadrupole moment [Fig. 2(d)] are increasing in the general direction of the experimental result, these poorly-converged results do not permit meaningful, quantitative comparison.

However, let us now take the dimensionless ratio of the form defined in (3) for these observables, namely, $B(E2; 3/2^- \rightarrow 1/2^-)/[eQ(3/2^-)]^2$, with the result shown in Fig. 2(g). We find a near complete elimination of the $\hbar\omega$ dependence, at the higher $N_{\max}$ shown, as well as a radical compression of the curves for successive $N_{\max}$. Calibrating to the known ground-state quadrupole moment [19] gives the scale shown at far right [Fig. 2 (bottom)]. An estimated ratio of $B(E2; 3/2^- \rightarrow 1/2^-)/[eQ(3/2^-)]^2 \approx 0.50$ yields $B(E2; 3/2^- \rightarrow 1/2^-) \approx 8\,e^2\mathrm{fm}^4$. The predicted ratio $B(E2)/(eQ)^2$ is consistent, to within uncertainties, with the experimental ratio of 0.52(3), and the resulting $B(E2)$ is similarly within uncertainties of the experimental strength.

From a physical viewpoint, the close-lying $3/2^-$ ground state and $1/2^-$ excited state in $^7$Li are interpreted as members of a $K = 1/2$ rotational band [38], where the energy order is inverted due to Coriolis staggering [3]. For context, the calculated and experimental excitation energies of the yrast levels are shown in Fig. 3(a) (see also Fig. 3 of Ref. [17] and Fig. 2 of Ref. [11] for more extensive calculated level schemes, of the mirror nuclide $^7$Be, obtained with the same Daejeon16 interaction). The rotational model yields $B(E2; 3/2_{K=1/2} \rightarrow 1/2_{K=1/2})/[eQ(3/2_{K=1/2})]^2 \approx 0.497$, indicated by the asterisk in Fig. 2(g). We are thus seeing close consistency between *ab initio* theory and experiment, both of which are well-explained by a simple rotational picture [13].

To explore the dependence upon internucleon interaction, let us consider the results for these same observables, but from calculations based on the JISP16 [Fig. 2 (center)] and LENPIC Fig. 2 (right)] internucleon interactions. The phenomenological JISP16 interaction [39] is obtained by $J$-matrix inverse scattering from nucleon-nucleon scattering data, and, like Daejeon16, adjusted via a phase-shift equivalent transformation to better describe nuclei with $A \leq 16$. The LENPIC interaction [40, 41] is a modern chiral EFT interaction (we specifically take the two-body part, at N$^2$LO, with a semi-local coordinate-space regulator of length scale $R = 1\,\mathrm{fm}$, and, for purposes of illustration, use the bare interaction with no SRG transformation).

For the $B(E2)$ itself, there is at best minimal suggestion of convergence, or shouldering, in the JISP16 results [Fig. 2(b)], and essentially no sign of convergence in the LENPIC results [Fig. 2(c)]. The same may be said for the computed quadrupole moments [Fig. 2(e,f)]. Nonetheless, taking the dimensionless ratio $B(E2)/(eQ)^2$ [Fig. 2(h,i)] again leads to a rapidly convergent quantity, from which the $\hbar\omega$ dependence has largely been eliminated, and the changes with successive $N_{\mathrm{max}}$ rapidly decrease. The resulting values for the ratio, as obtained with these interactions, is closely consistent both with that obtained from the Daejeon16 interaction [Fig. 2(g)] and with experiment.

Predictions for this same quadrupole moment and transition matrix element in $^7$Li have previously been reported [28] from *ab initio* Green's function Monte Carlo (GFMC) [37] calculations, based on the Argonne $v_{18}$ (AV18) two-nucleon [42] and Illinois-7 (IL7) three-nucleon [43] potentials. These predictions, shown as crosses in Fig. 2 (left), are subject to Monte Carlo statistical errors, so the calculational uncertainties are of a qualitatively different nature from those entering into the NCCI calculations. In particular, the GFMC calculated values for the $E2$ transition strength [Fig. 2(a)] and quadrupole moment [Fig. 2(d)] may meaningfully be compared directly with experiment, without taking a ratio to can-

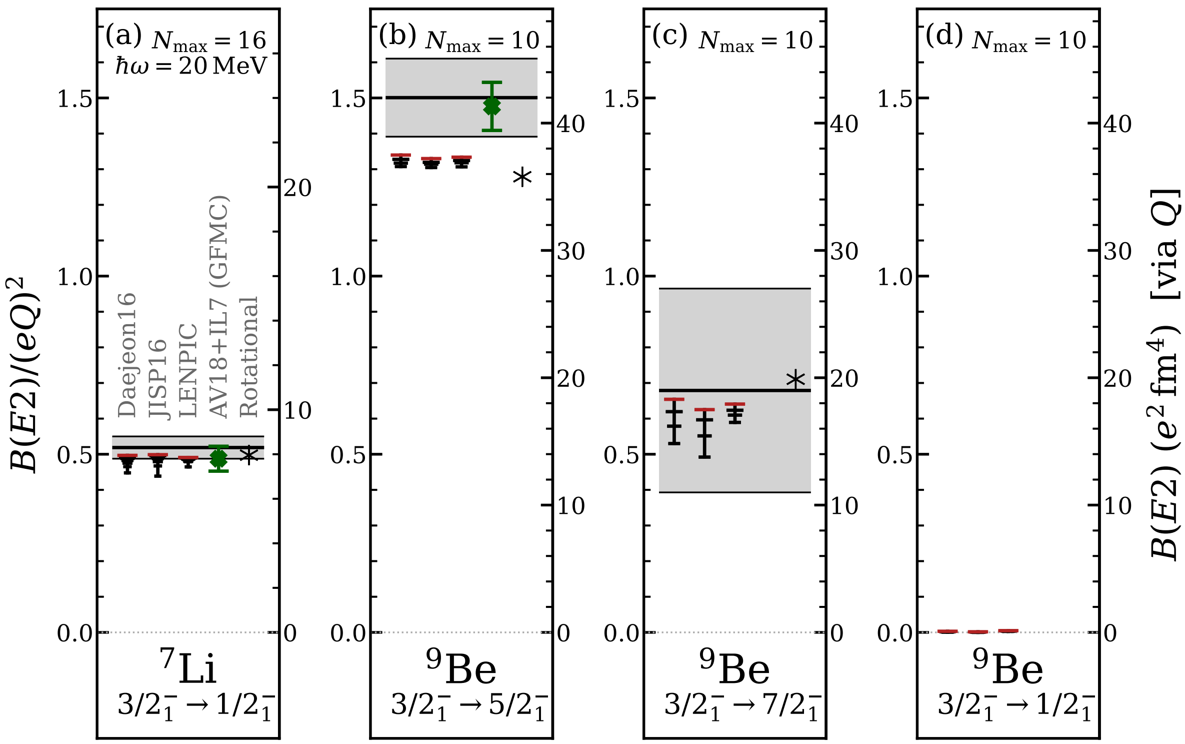


FIG. 4. Calculated ratios of the form $B(E2)/(eQ)^2$, for excitation to low-lying states in $^7$Li and $^9$Be, obtained with the Daejeon16, JISP16, and LENPIC interactions (from left to right, for each transition). Calculated values are shown at fixed $\hbar\omega = 20\,\mathrm{MeV}$ and varying $N_{\max}$ (increasing symbol size), from $N_{\max} = 4$ to the maximum value indicated (at top). When calibrated to the experimental quadrupole moment [19], this ratio provides an estimate for the absolute $B(E2)$ (scale at right). Experimental results [19–21] are shown (horizontal line and error band) where available, as are the GFMC AV18+IL7 predictions [28] (crosses) and rotational ratios (asterisks).

cel truncation errors, and we see agreement within uncertainties in both cases. Nonetheless, for comparison with the NCCI results, we may recast these GFMC results as a ratio $B(E2)/(eQ)^2$ [cross in Fig. 2(g)], where we find consistency with experiment (again), but now also with the NCCI predictions for the ratio.

To provide for convenient comparison across calculations and (in the following discussion) transitions, we take a “slice” through these NCCI results in Fig. 4(a), which shows convergence with $N_{\max}$ at fixed $\hbar\omega$ (chosen as $\hbar\omega = 20\,\mathrm{MeV}$, based on the approximate location of the variational energy minimum for the ground state, although this location varies somewhat by nuclide and interaction). We may again readily compare the NCCI results with experiment (horizontal lines and shaded error bands), GFMC AV18+IL7 predictions

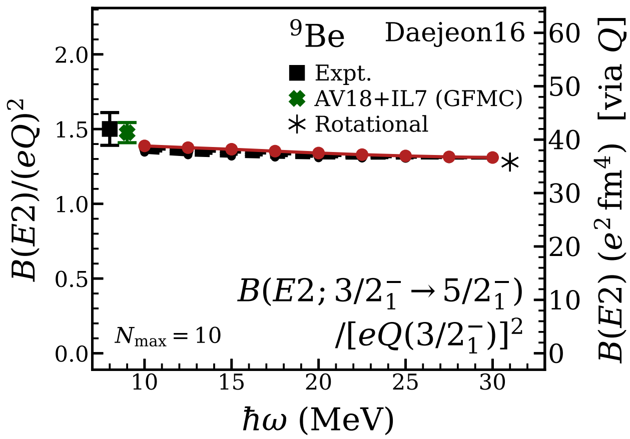


FIG. 5. Convergence of the *ab initio* NCCI calculated dimensionless ratio $B(E2)/(eQ)^2$, for $^9$Be, constructed from the $3/2^- \rightarrow 5/2^-$ $E2$ strength and the electric quadrupole moment of the $3/2^-$ ground state. Results are shown for the Daejeon16 interaction. When calibrated to the experimental quadrupole moment, the ratio provides a prediction for the absolute $B(E2)$ (scale at right). Calculated values are shown as functions of the basis parameter $\hbar\omega$, for successive even value of $N_{\mathrm{max}}$ (increasing symbol size and longer dashing), from $N_{\mathrm{max}} = 4$ (short dashed curves) to 10 (solid curves). For comparison, the experimental ratio [19, 21] (square), GFMC AV18+IL7 prediction [28] (cross), and rotational ratio (asterisk) are also shown.

(crosses), and the rotational model (asterisks), where applicable.

In $^9$Be, the $E2$ transition from the $3/2^-$ ground state to the $5/2^-$ excited state (a narrow resonance just above the neutron threshold, with a width of $\approx 0.8\,\mathrm{keV}$ [20]) is interpreted as an in-band transition within the ground-state ($K = 3/2$) rotational band [38]. For context, calculated and experimental excitation energies of the (normal-parity [44]) yrast levels of $^9$Be, including the $J = 3/2$, $5/2$, and $7/2$ members of the ground state $K = 3/2$ band and the excited $K = 1/2$ band head, are shown in Fig. 3(b) (see also Fig. 1 of Ref. [17] for a more extensive calculated level scheme, obtained with the same Daejeon16 interaction).

The dimensionless ratio $B(E2)/(eQ)^2$, as obtained with the Daejeon16 interaction, is shown in Fig. 5, and similar results are obtained with the other two interactions considered above, as summarized in Fig. 4(b). Again, taking the dimensionless ratio largely eliminates the $\hbar\omega$ dependence of the results and yields rapid convergence with respect to $N_{\mathrm{max}}$. Calibrating to the known ground-state quadrupole moment [19] gives the scale shown at right. An estimated ratio of $B(E2; 3/2^- \rightarrow 5/2^-)/[eQ(3/2^-)]^2 \approx 1.3$–$1.4$ yields

$B(E2; 3/2^- \rightarrow 5/2^-) \approx 36$–$39\, e^2\text{fm}^4$. The NCCI results for this ratio (with all three interactions) lie just below the uncertainty ranges for the experimental ratio (square) and for the GFMC AV18+IL7 predictions (cross), and just above the ratio of $B(E2; 3/2_{K=3/2} \rightarrow 5/2_{K=3/2})/[eQ(3/2_{K=3/2})]^2 \approx 1.279$ for an ideal rotational description (asterisk).

For the in-band transition to the $7/2^-$ band member in $^9$Be [Fig. 4(c)], the *ab initio* predictions for the ratio $B(E2; 3/2^- \rightarrow 7/2^-)/[eQ(3/2^-)]^2$ are consistent across choice of interaction and closely agree with the rotational value $B(E2; 3/2_{K=3/2} \rightarrow 7/2_{K=3/2})/[eQ(3/2_{K=3/2})]^2 \approx 0.711$, while lying well within generous experimental uncertainties.

The strength of any interband $E2$ transition to the $1/2^-$ band head is experimentally unknown [21]. However, the present NCCI calculations give a ratio $B(E2)/(eQ)^2$ which is essentially vanishing on the scale of Fig. 4(d). The calculated ratios $B(E2; 3/2^- \rightarrow 1/2^-)/[eQ(3/2^-)]^2 \lesssim 0.005$ suggest $B(E2; 3/2^- \rightarrow 1/2^-) \lesssim 0.2\, e^2\text{fm}^4$. In a rotational description, the interband $E2$ strength depends upon the interband intrinsic $E2$ matrix element [1–3], and a limit on the ratio $B(E2)/(eQ)^2$ may be translated, through appropriate Clebsch-Gordan factors, into a limit on the ratio of in-band and interband intrinsic matrix elements.

## IV. PREDICTIONS FOR $^8$Li AND $^9$Li

Returning to the $2^+ \rightarrow 1^+$ transition in $^8$Li, the NCCI calculations for the relevant observables are shown in Fig. 6. For context, calculated and experimental excitation energies of low-lying levels in $^8$Li are shown in Fig. 7(a). We again compare results obtained for the Daejeon16 [Fig. 6(a)], JISP16 [Fig. 6(b)], and LENPIC [Fig. 6(c)] interactions.

Focusing first on the Daejeon16 results [Fig. 6(a)], we see that taking the dimensionless ratio $B(E2; 2^+ \rightarrow 1^+)/[eQ(2^+)]^2$ rapidly eliminates the $\hbar\omega$ and $N_{\max}$ dependence, at the scale shown, even for modest $N_{\max}$. Calibrating to the known $Q(2^+) = +3.14(2)\,\text{fm}^2$ [19] yields the scale at far right. A ratio of $\approx 0.18$, taken in conjunction with this quadrupole moment, yields an estimated $B(E2; 2^+ \rightarrow 1^+) \approx 1.8\, e^2\text{fm}^4$.

For the JISP16 interaction [Fig. 6(b)], the dimensionless ratio exhibits greater $\hbar\omega$ dependence than found for Daejeon16 [Fig. 6(a)], especially for lower $N_{\max}$. Nonetheless, it appears to robustly converge towards a result, $B(E2; 2^+ \rightarrow 1^+)/[eQ(2^+)]^2 \approx 0.10$, in this case lower by nearly a factor of two than obtained for Daejeon16.

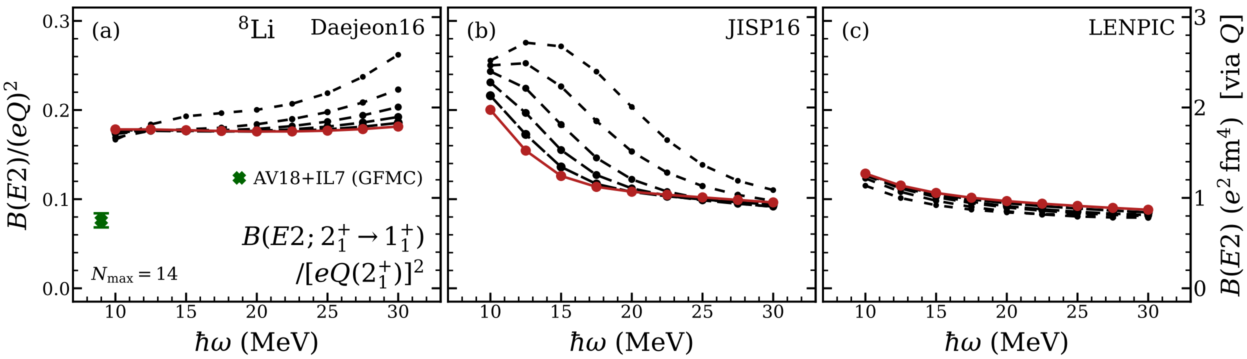


FIG. 6. Convergence of the *ab initio* NCCI calculated dimensionless ratio $B(E2)/(eQ)^2$, for $^8$Li, constructed from the $2^+ \rightarrow 1^+$ $E2$ strength and the electric quadrupole moment of the $2^+$ ground state. Results are shown for the (a) Daejeon16, (b) JISP16, and (c) LENPIC interactions. When calibrated to the experimental quadrupole moment, the ratio provides a prediction for the absolute $B(E2)$ (scale at right). Calculated values are shown as functions of the basis parameter $\hbar\omega$, for successive even value of $N_{\mathrm{max}}$ (increasing symbol size and longer dashing), from $N_{\mathrm{max}} = 4$ (short dashed curves) to 14 (solid curves). For comparison, the GFMC AV18+IL7 prediction [28] (crosse) is shown, while the experimental ratio [19, 21], corresponding to the reported $E2$ strength of $55(15)\,e^2\mathrm{fm}^4$ [26], lies off scale.

For the LENPIC interaction [Fig. 6(c)], taking the dimensionless ratio tames the $\hbar\omega$ dependence, indeed, more effectively than for JISP16 [Fig. 6(b)]. There is still a slow but steady increase with $N_{\mathrm{max}}$ over much of the $\hbar\omega$ range. Nonetheless, with this caveat, the calculated ratio is again in the vicinity of 0.10.[1]

Thus, as summarized in Fig. 8(a), the NCCI predictions show the ratio $B(E2)/(eQ)^2$ to depend upon the choice of interaction, varying within the range $\approx$ 0.1–0.2. By way of comparison, GFMC calculation [28] gives $B(E2;2^+ \rightarrow 1^+) = 0.83(7)\,e^2\mathrm{fm}^4$ and $Q(2^+) = +3.3(1)\,\mathrm{fm}^2$, which, recast as a ratio, yield $B(E2;2^+ \rightarrow 1^+)/[eQ(2^+)]^2 = 0.076(8)$, similar in scale to and marginally below these NCCI estimates.

That the *ab initio* predictions for the $2^+ \rightarrow 1^+$ transition, and in particular for the ratio to the squared quadrupole moment, show a greater dependence upon the internucleon

[1] The earlier NCCI calculations of Maris *et al.* [45], based on the chiral N$^3$LO two-nucleon interaction of Entem and Machleidt [31], together with the N$^2$LO three-nucleon interaction of Navrátil [46], carried out using a basis with $N_{\mathrm{max}} = 8$ and $\hbar\omega = 13\,\mathrm{MeV}$, and calculated with an Okubo-Lee-Suzuki [47, 48] renormalized effective interaction, give $Q(2^+) = 2.648\,\mathrm{fm}^2$ and $B(E2;2^+ \rightarrow 1^+) = 0.714\,e^2\mathrm{fm}^4$, similarly yielding a ratio of $B(E2;2^+ \rightarrow 1^+)/[eQ(2^+)]^2 \approx 0.10$.

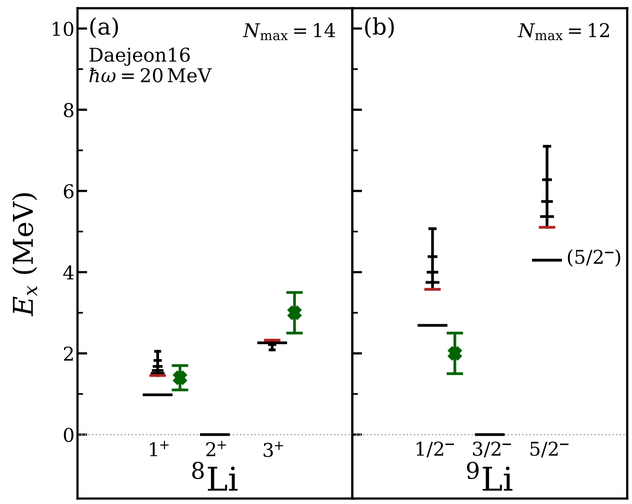


FIG. 7. Calculated excitation energies of low-lying states in (a) $^8$Li and (b) $^9$Li, with angular momentum and parity as indicated at bottom, as obtained with the Daejeon16 interaction. Calculated values are shown at fixed $\hbar\omega = 20\,\mathrm{MeV}$ and varying $N_{\max}$ (increasing symbol size), from $N_{\max} = 4$ to the maximum value indicated (at top). Experimental energies [21] are shown (horizontal line and error band) where available, as are the GFMC AV18+IL7 predictions [28] (crosses) (see Table III of Ref. [37]).

interaction than found above (Sec. III) for the in-band rotational transitions in $^7$Li and $^9$Be is perhaps not surprising. One may take the perspective that the $E2$ ratio is not "constrained" by the symmetry considerations which apply to in-band transitions in an axially symmetric rotor or, perhaps, an Elliott SU(3) rotor [38, 49, 50]. If the $2^+ \rightarrow 1^+$ transition is taken to be an interband transition, rather, it is sensitive to the detailed microscopic structure of rotational intrinsic states. More generally, the transition involved is (predicted to be) a weak ("noncollective") transition, which might be expected to be sensitive, *e.g.*, in a shell model picture, to admixtures of different $p$-shell configurations favored by the different interactions.

However, taken in conjunction with the known $Q(2^+) = +3.14(2)\,\mathrm{fm}^2$ [19], these *ab initio* results are all consistent with a modest strength of $\approx 1$–$2\,e^2\mathrm{fm}^4$ for the $2^+ \rightarrow 1^+$ transition, more than an order of magnitude smaller than the experimental value of $55(15)\,e^2\mathrm{fm}^4$ [21, 26]. It is thus of particular interest to obtain confirmation of this reported strength.

It is interesting to contrast the results for this $2^+ \rightarrow 1^+$ transition in $^8$Li with the results for the ostensibly in-band $2^+ \rightarrow 3^+$ transition, shown in Fig. 8(b). In a rotational description, the $3^+$ second excited state (a narrow resonance at 2.2 MeV, just above the

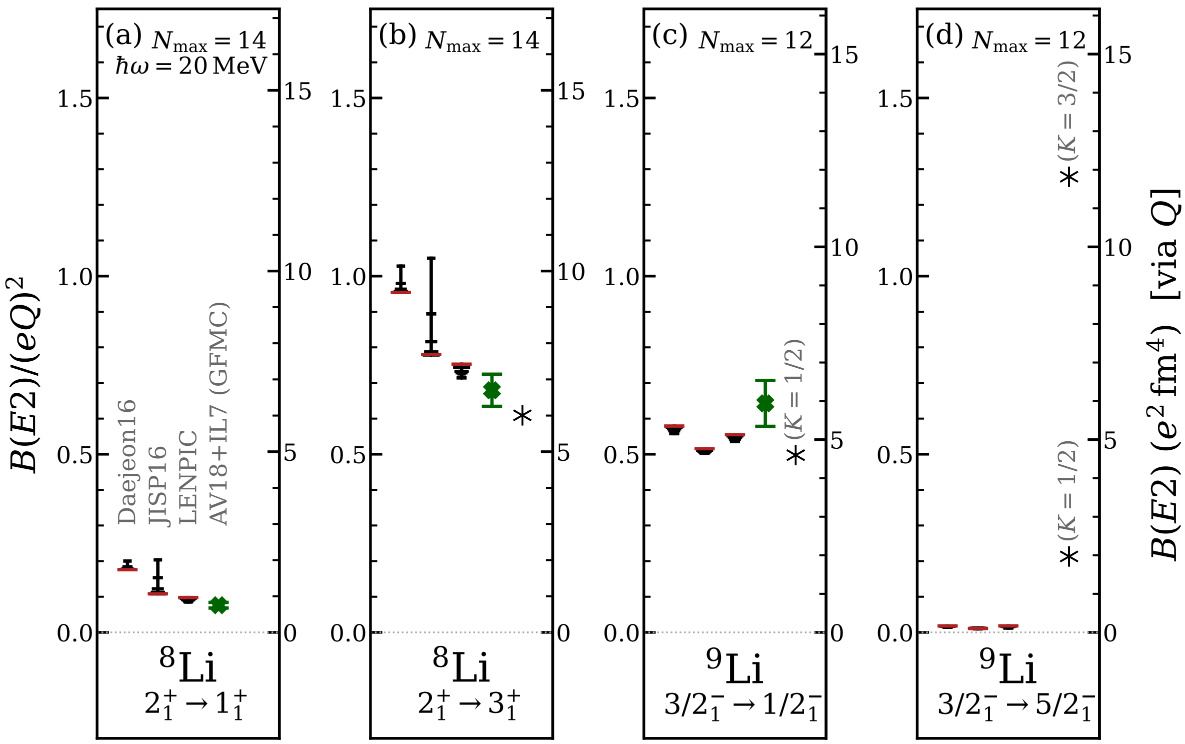


FIG. 8. Calculated ratios of the form $B(E2)/(eQ)^2$, for excitation to low-lying states in $^8$Li and $^9$Li, obtained with the Daejeon16, JISP16, and LENPIC interactions (from left to right, for each transition). Calculated values are shown at fixed $\hbar\omega = 20\,\mathrm{MeV}$ and varying $N_{\max}$ (increasing symbol size), from $N_{\max} = 4$ to the maximum value indicated (at top). When calibrated to the experimental quadrupole moment [19], this ratio provides an estimate for the absolute $B(E2)$ (scale at right). Experimental results [19, 21] are shown (horizontal line and error band) where available (the $^8$Li $2^+ \rightarrow 1^+$ transition strength lies off scale), as are the GFMC AV18+IL7 predictions [28] (crosses) and rotational ratios (asterisks).

neutron separation threshold) is naturally taken as a member of the $K = 2$ ground state band. Experimentally, only the $M1$ partial decay width is known [21], from a $^7$Li$(n,\gamma)$ measurement [51], while a Coulomb excitation measurement for the $E2$ strength would require neutron detection. The NCCI calculations, as obtained with the three different interactions, suggest ratios $B(E2; 2^+ \rightarrow 3^+)/[eQ(2^+)]^2$ in the range $\approx$ 0.7–1.0, with the GFMC prediction [28] coming in at the low end of this range, and the rotational ratio of $\approx 0.609$ coming lower still. In conjunction with the known quadrupole moment, the NCCI calculated ratios yield a comparatively collective $B(E2; 2^+ \rightarrow 3^+)$ of $\approx$ 7–10 $e^2\mathrm{fm}^4$.

We conclude with NCCI predictions for the unmeasured $E2$ strengths from the $3/2^-$

ground state of $^9$Li to the first two excited states [21]. The only excited state below the neutron threshold is a $1/2^-$ state at $\approx 2.7\,\mathrm{MeV}$, while a resonance at $\approx 4.3\,\mathrm{MeV}$, just above the neutron threshold, has tentative $(5/2^-)$ assignment. This low-lying spectrum is consistent with the level ordering obtained in the present NCCI calculations. Calculated and experimental excitation energies are shown in Fig. 7(b).

The NCCI predictions for the dimensionless ratio $B(E2; 3/2^- \rightarrow 1/2^-)/[eQ(3/2^-)]^2$, shown in Fig. 8(c), are robustly converged with respect to basis truncation. The ratio is found to depend modestly upon interaction, within the range $\approx 0.5$–$0.6$. Calibrating to the known ground-state quadrupole moment [19] yields strengths, depending upon interaction, in the range $B(E2; 3/2^- \rightarrow 1/2^-) \approx 4.6$–$5.5\,e^2\mathrm{fm}^4$. The GFMC AV18+IL7 predictions [28], recast as a ratio, give 0.64(6), which is roughly consistent with the ratios found in the NCCI calculations. However, on an absolute scale, the GFMC calculated $Q(3/2^-) = -2.3(1)\,\mathrm{fm}^2$ underpredicts the experimental quadrupole moment by $\approx 24\%$, and the calculated $B(E2; 3/2^- \rightarrow 1/2^-) = 3.40(17)\,e^2\mathrm{fm}^4$ is thus correspondingly lower than the above estimates.

In a rotational description, it is not *a priori* obvious whether this transition should be interpreted as an in-band transition within a Coriolis-staggered $K = 1/2$ band, as in $^7$Li (Sec. III), or an interband transition between $K = 3/2$ ground state and $K = 1/2$ excited band heads. The former interpretation would give an expected rotational ratio of $B(E2; 3/2_{K=1/2} \rightarrow 1/2_{K=1/2})/[eQ(3/2_{K=1/2})]^2 \approx 0.497$, as above for $^7$Li, while in the latter case the rotational prediction would depend on the ratio of interband and in-band intrinsic matrix elements. The *ab initio* results are roughly consistent with the $K = 1/2$ in-band interpretation.

For the transition to the $5/2^-$ state, the NCCI calculations, shown in Fig. 8(d), give $B(E2; 3/2^- \rightarrow 5/2^-)/[eQ(3/2^-)]^2 \approx 0.01$–$0.02$, depending upon choice of interaction, yielding a compartively weak $B(E2; 3/2^- \rightarrow 5/2^-) \approx 0.1$–$0.2\,e^2\mathrm{fm}^4$. The *ab initio* predicted ratio is not conducive to an interpretation of this transition as a rotational in-band transition, whether within a Coriolis-staggered $K = 1/2$ band, for which $B(E2; 3/2_{K=1/2} \rightarrow 5/2_{K=1/2})/[eQ(3/2_{K=1/2})]^2 \approx 0.213$, or within a $K = 3/2$ band built on the ground state, for which $B(E2; 3/2_{K=3/2} \rightarrow 5/2_{K=3/2})/[eQ(3/2_{K=3/2})]^2 \approx 1.279$.

## V. CONCLUSION

Although meaningful, converged predictions for $E2$ observables are elusive in *ab initio* NCCI calculations, calculated $E2$ observables are correlated, presumably due to their common dependence on the truncation of the long-distance tails of the wave functions. For the ground-state quadrupole moment and low-lying transitions, we demonstrate that much of this systematic truncation error cancels out in dimensionless ratios of the form $B(E2)/(eQ)^2$, allowing robust predictions to be obtained. Calibrating to the known ground-state quadrupole moment then provides an $E2$ strength estimate on an absolute scale.

For the rotational in-band transitions in $^7$Li and $^9$Be, there is general agreement, in the $B(E2)/(eQ)^2$ ratios, between the predictions obtained across several choices for the internucleon interaction. These calculated values, like the experimental ratios and GFMC predictions, are approximately consistent with the simple axial rotor model, and calibrating to the ground-state quadrupole moment reproduces the experimentally observed $E2$ enhancement. For the $2^+ \rightarrow 1^+$ transition in $^8$Li, which is not naturally interpreted as a rotational in-band transition, robust *ab initio* predictions are made for the ratio $B(E2)/(eQ)^2$, showing modest dependence on the choice of internucleon interaction, and reinforcing the severe tension between *ab initio* theory [28] and experiment [21, 26] for this transition. Finally, we provide robust *ab initio* predictions for the ratio $B(E2)/(eQ)^2$, and thus, by normalization to the experimental ground state quadrupole moment, estimates for unmeasured $E2$ strengths to the low-lying $3^+$ resonance of $^8$Li and to low-lying states of $^9$Li.

## ACKNOWLEDGMENTS

We thank Tan Ahn, Samuel L. Henderson, Pieter Maris, and Anna E. McCoy for valuable discussions, James P. Vary, Ik Jae Shin, and Youngman Kim for sharing illuminating results on ratios of observables, and Colin V. Coane, Jakub Herko, and Zhou Zhou for comments on the manuscript. This material is based upon work supported by the U.S. Department of Energy, Office of Science, under Award No. DE-FG02-95ER40934. This research used resources of the National Energy Research Scientific Computing Center (NERSC), a DOE Office of Science User Facility supported by the Office of Science of the U.S. Department of Energy under Contract No. DE-AC02-05CH11231, using NERSC award NP-ERCAP0020422.

---

[1] A. Bohr and B. R. Mottelson, *Nuclear Structure*, Vol. 2 (World Scientific, Singapore, 1998).

[2] R. F. Casten, *Nuclear Structure from a Simple Perspective*, 2nd ed., Oxford Studies in Nuclear Physics No. 23 (Oxford University Press, Oxford, 2000).

[3] D. J. Rowe, *Nuclear Collective Motion: Models and Theory* (World Scientific, Singapore, 2010).

[4] S. K. Bogner, R. J. Furnstahl, P. Maris, R. J. Perry, A. Schwenk, and J. Vary, Convergence in the no-core shell model with low-momentum two-nucleon interactions, Nucl. Phys. A **801**, 21 (2008).

[5] P. Maris and J. P. Vary, *Ab initio* nuclear structure calculations of $p$-shell nuclei with JISP16, Int. J. Mod. Phys. E **22**, 1330016 (2013).

[6] D. Odell, T. Papenbrock, and L. Platter, Infrared extrapolations of quadrupole moments and transitions, Phys. Rev. C **93**, 044331 (2016).

[7] B. R. Barrett, P. Navrátil, and J. P. Vary, *Ab initio* no core shell model, Prog. Part. Nucl. Phys. **69**, 131 (2013).

[8] R. Roth and P. Navrátil, *Ab initio* study of $^{40}$Ca with an importance-truncated no-core shell model, Phys. Rev. Lett. **99**, 092501 (2007).

[9] T. Dytrych, K. D. Sviratcheva, J. P. Draayer, C. Bahri, and J. P. Vary, *Ab initio* symplectic no-core shell model, J. Phys. G **35**, 123101 (2008); T. Dytrych, P. Maris, K. D. Launey, J. P. Draayer, J. P. Vary, D. Langr, E. Saule, M. A. Caprio, U. Catalyurek, and M. Sosonkina, Efficacy of the SU(3) scheme for *ab initio* large-scale calculations beyond the lightest nuclei, Comput. Phys. Commun. **207**, 202 (2016).

[10] M. Vorabbi, P. Navrátil, S. Quaglioni, and G. Hupin, $^7$Be and $^7$Li nuclei within the no-core shell model with continuum, Phys. Rev. C **100**, 024304 (2019).

[11] A. E. McCoy, M. A. Caprio, T. Dytrych, and P. J. Fasano, Emergent $\mathrm{Sp}(3,\mathbb{R})$ dynamical symmetry in the nuclear many-body system from an *ab initio* description, Phys. Rev. Lett. **125**, 102505 (2020).

[12] P. J. Fasano, Ch. Constantinou, M. A. Caprio, P. Maris, and J. P. Vary, Natural orbitals for the *ab initio* no-core configuration interaction approach, Phys. Rev. C **105**, 054301 (2022).

[13] M. A. Caprio, P. Maris, and J. P. Vary, Emergence of rotational bands in *ab initio* no-core configuration interaction calculations of light nuclei, Phys. Lett. B **719**, 179 (2013); P. Maris, M. A. Caprio, and J. P. Vary, Emergence of rotational bands in *ab initio* no-core configuration interaction calculations of the Be isotopes, Phys. Rev. C **91**, 014310 (2015); Erratum: Emergence of rotational bands in *ab initio* no-core configuration interaction calculations of the Be isotopes, Phys. Rev. C **99**, 029902(E) (2019).

[14] A. Calci and R. Roth, Sensitivities and correlations of nuclear structure observables emerging from chiral interactions, Phys. Rev. C **94**, 014322 (2016).

[15] S. L. Henderson, T. Ahn, M. A. Caprio, P. J. Fasano, A. Simon, W. Tan, P. O'Malley, J. Allen, D. W. Bardayan, D. Blankstein, B. Frentz, M. R. Hall, J. J. Kolata, A. E. McCoy, S. Moylan, C. S. Reingold, S. Y. Strauss, and R. O. Torres-Isea, First measurement of the $B(E2;3/2^- \rightarrow 1/2^-)$ transition strength in $^7$Be: Testing *ab initio* predictions for $A = 7$ nuclei, Phys. Rev. C **99**, 064320 (2019).

[16] M. A. Caprio, P. J. Fasano, A. E. McCoy, P. Maris, and J. P. Vary, *Ab initio* rotation in $^{10}$Be, Bulg. J. Phys. **46**, 445 (2019).

[17] M. A. Caprio, P. J. Fasano, P. Maris, A. E. McCoy, and J. P. Vary, Probing *ab initio* emergence of nuclear rotation, Eur. Phys. J. A **56**, 120 (2020).

[18] M. A. Caprio, P. J. Fasano, P. Maris, and A. E. McCoy, Quadrupole moments and proton-neutron structure in $p$-shell mirror nuclei, Phys. Rev. C **104**, 034319 (2021).

[19] N. J. Stone, Table of nuclear electric quadrupole moments, At. Data Nucl. Data Tables **111-112**, 1 (2016).

[20] D. R. Tilley, C. M. Cheves, J. L. Godwin, G. M. Hale, H. M. Hofmann, J. H. Kelley, C. G. Sheu, and H. R. Weller, Energy levels of light nuclei $A = 5, 6, 7$, Nucl. Phys. A **708**, 3 (2002).

[21] D. R. Tilley, J. H. Kelley, J. L. Godwin, D. J. Millener, J. E. Purcell, C. G. Sheu, and H. R. Weller, Energy levels of light nuclei $A = 8$, 9, 10, Nucl. Phys. A **745**, 155 (2004).

[22] J. Kelley, E. Kwan, J. E. Purcell, C. G. Sheu, and H. R. Weller, Energy levels of light nuclei $A = 11$, Nucl. Phys. A **880**, 88 (2012).

[23] J. Kelley, J. E. Purcell, and C. G. Sheu, Energy levels of light nuclei $A = 12$, Nucl. Phys. A **968**, 71 (2017).

[24] F. Ajzenberg-Selove, Energy levels of light nuclei $A = 13$–15, Nucl. Phys. A **523**, 1 (1991).

[25] R. Neugart and G. Neyens, Nuclear moments, in *The Euroschool Lectures on Physics with*

*Exotic Beams, Vol. II*, Lecture Notes in Physics, Vol. 700, edited by J. Al-Khalili and E. Roeckl (Springer-Verlag, Berlin, 2006) p. 135.

[26] J. A. Brown, F. D. Becchetti, J. W. Jänecke, K. Ashktorab, D. A. Roberts, J. J. Kolata, R. J. Smith, K. Lamkin, and R. E. Warner, Coulomb excitation of $^8$Li, Phys. Rev. Lett. **66**, 2452 (1991).

[27] V. F. Weisskopf, Radiative transition probabilities in nuclei, Phys. Rev. **83**, 1073 (1951).

[28] S. Pastore, S. C. Pieper, R. Schiavilla, and R. B. Wiringa, Quantum Monte Carlo calculations of electromagnetic moments and transitions in $A \leq 9$ nuclei with meson-exchange currents derived from chiral effective field theory, Phys. Rev. C **87**, 035503 (2013).

[29] J. Suhonen, *From Nucleons to Nucleus* (Springer-Verlag, Berlin, 2007).

[30] A. M. Shirokov, I. J. Shin, Y. Kim, M. Sosonkina, P. Maris, and J. P. Vary, N3LO $NN$ interaction adjusted to light nuclei in *ab exitu* approach, Phys. Lett. B **761**, 87 (2016).

[31] D. R. Entem and R. Machleidt, Accurate charge-dependent nucleon-nucleon potential at fourth order of chiral perturbation theory, Phys. Rev. C **68**, 041001(R) (2003).

[32] S. K. Bogner, R. J. Furnstahl, and R. J. Perry, Similarity renormalization group for nucleon-nucleon interactions, Phys. Rev. C **75**, 061001(R) (2007).

[33] H. M. Aktulga, C. Yang, E. G. Ng, P. Maris, and J. P. Vary, Improving the scalability of symmetric iterative eigensolver for multi-core platforms, Concurrency Computat.: Pract. Exper. **26**, 2631 (2014).

[34] M. Shao, H. M. Aktulga, C. Yang, E. G. Ng, P. Maris, and J. P. Vary, Accelerating nuclear configuration interaction calculations through a preconditioned block iterative eigensolver, Comput. Phys. Commun. **222**, 1 (2018).

[35] B. G. Cook, P. J. Fasano, P. Maris, C. Yang, and D. Oryspayev, Accelerating quantum many-body configuration interaction with directives, in *Accelerator Programming Using Directives*, Lect. Notes Comput. Sci., Vol. 13194, edited by S. Bhalachandra, C. Daley, and V. Melesse Vergara (Springer-Verlag, 2022) pp. 112–132.

[36] See Supplemental Material at http://xxxxxxxx for comprehensive plots and tabulations of the calculated observables, as functions of $N_{\mathrm{max}}$ and $\hbar\omega$.

[37] J. Carlson, S. Gandolfi, F. Pederiva, S. C. Pieper, R. Schiavilla, K. E. Schmidt, and R. B. Wiringa, Quantum Monte Carlo methods for nuclear physics, Rev. Mod. Phys. **87**, 1067 (2015).

[38] D. J. Millener, Structure of unstable light nuclei, Nucl. Phys. A **693**, 394 (2001); Hypernuclear

gamma-ray spectroscopy and the structure of $p$-shell nuclei and hypernuclei, in *Topics in Strangeness Nuclear Physics*, Lecture Notes in Physics, Vol. 724, edited by P. Bydžovský, J. Mareš, and A. Gal (Springer, Berlin, 2007) pp. 31–79.

[39] A. M. Shirokov, J. P. Vary, A. I. Mazur, and T. A. Weber, Realistic nuclear Hamiltonian: *Ab exitu* approach, Phys. Lett. B **644**, 33 (2007).

[40] E. Epelbaum, H. Krebs, and U.-G. Meißner, Precision nucleon-nucleon potential at fifth order in the chiral expansion, Phys. Rev. Lett. **115**, 122301 (2015).

[41] E. Epelbaum, H. Krebs, and U.-G. Meißner, Improved chiral nucleon-nucleon potential up to next-to-next-to-next-to-leading order, Eur. Phys. J. A **51**, 53 (2015).

[42] R. B. Wiringa, V. G. J. Stoks, and R. Schiavilla, Accurate nucleon-nucleon potential with charge-independence breaking, Phys. Rev. C **51**, 38 (1995).

[43] S. C. Pieper, V. R. Pandharipande, R. B. Wiringa, and J. Carlson, Realistic models of pion-exchange three-nucleon interactions, Phys. Rev. C **64**, 014001 (2001).

[44] A. M. Lane, Reduced widths of individual nuclear energy levels, Rev. Mod. Phys. **32**, 519 (1960).

[45] P. Maris, J. P. Vary, and P. Navrátil, Structure of $A = 7$–8 nuclei with two- plus three-nucleon interactions from chiral effective field theory, Phys. Rev. C **87**, 014327 (2013).

[46] P. Navrátil, Local three-nucleon interaction from chiral effective field theory, Few-Body Syst. **41**, 117 (2007).

[47] S. Ôkubo, Diagonalization of Hamiltonian and Tamm-Dancoff equation, Prog. Theor. Phys. **12**, 603 (1954).

[48] K. Suzuki and S. Y. Lee, Convergent theory for effective interaction in nuclei, Prog. Theor. Phys. **64**, 2091 (1980).

[49] J. P. Elliott, Collective motion in the nuclear shell model. I. Classification schemes for states of mixed configurations, Proc. R. Soc. London A **245**, 128 (1958); Collective motion in the nuclear shell model. II. The introduction of intrinsic wave functions, Proc. R. Soc. London A **245**, 562 (1958); J. P. Elliott and M. Harvey, Collective motion in the nuclear shell model. III. The calculation of spectra, Proc. R. Soc. London A **272**, 557 (1963); J. P. Elliott and C. E. Wilsdon, Collective motion in the nuclear shell model. IV. Odd-mass nuclei in the *sd* shell, Proc. R. Soc. London A **302**, 509 (1968).

[50] M. Harvey, The nuclear $SU_3$ model, in *Adv. Nucl. Phys.*, Vol. 1, edited by M. Baranger and

E. Vogt (Plenum, New York, 1968) p. 67.

[51] M. Heil, F. Kappeler, M. Wiescher, and A. Mengoni, The $(n, \gamma)$ cross section of $^7$Li, Astrophys. J. **507**, 997 (1998).